

Electrostatic Turbulence and Transport in the Velocity Shear Layer of a Reversed Field Pinch Plasma

V. Antoni, R. Cavazzana, D. Desideri, E. Martines, G. Serianni, and L. Tramontin

Consorzio RFX, corso Stati Uniti 4, 35127 Padova, Italy

(Received 14 November 1997)

The electrostatic turbulence in the edge plasma of the RFX reversed field pinch experiment has been studied using Langmuir probes and a homodyne reflectometer. The radial particle flux driven by electrostatic fluctuations has been measured in the region where a double $\mathbf{E} \times \mathbf{B}$ velocity shear layer occurs. It is found that almost 100% of the particle flux at the edge is driven by electrostatic fluctuations. The naturally occurring $\mathbf{E} \times \mathbf{B}$ velocity shear has been shown to be close to that required by the Biglari-Diamond-Terry criterion for turbulence radial decorrelation. [S0031-9007(98)06091-8]

PACS numbers: 52.25.Fi, 52.35.Ra, 52.55.Hc, 52.70.Ds

Plasmas confined in reversed field pinch (RFP) configurations are self-organized systems characterized by strong magnetic and electrostatic fluctuations, which are believed to determine the anomalous transport of particles and energy. In particular, the particle flux in the edge region has been found to be mainly driven by electrostatic fluctuations in most RFP experiments [1]. This evidence was already noted to bear some analogies with results from tokamaks and stellarators [2]. The analogy with tokamaks and stellarators has been recently reinforced by the observation of a naturally occurring velocity shear layer at the edge [3,4] similar to that observed in those configurations [5], and by the spontaneous occurrence of regimes of improved particle confinement, possibly associated to modifications of this velocity shear [6]. These observations suggest the possibility of a turbulence decorrelation mechanism induced by $\mathbf{E} \times \mathbf{B}$ velocity shear [7], like that playing a role in the H mode observed in tokamaks and stellarators [8]. In this Letter the electrostatic particle transport in the RFX reversed field pinch experiment is addressed and the relationship with the $\mathbf{E} \times \mathbf{B}$ velocity shear discussed. It is found that the naturally occurring velocity shear at the edge is close to that required for turbulence radial decorrelation and affects the fluctuation properties.

RFX is a reversed field pinch device with major radius $R = 2$ m and minor radius $a = 0.457$ m. The results reported herein have been obtained at a reduced plasma current of 300–400 kA and core electron density of about $3.5 \times 10^{19} \text{ m}^{-3}$. The electron density profile in the plasma core is generally flat or hollow at higher density, with a strong gradient at the edge.

A set of Langmuir probes has been used to measure the radial profiles of plasma potential and electron density and the properties of the electrostatic fluctuations. The system consists of a boron nitride head equipped with graphite pins flush with the head surface, having a diameter of 2 mm. The pin surface is oriented at 45° with respect to the magnetic field. In this campaign 5 pins were used, all located 2.2 mm right behind the head tip. The pins were aligned in the toroidal direction and at the same radial and poloidal

positions. It is worthwhile to remind that in the RFP configuration the magnetic field at the edge is approximately poloidal, so that the toroidal direction is perpendicular to the field, opposite to what happens in tokamaks. One of the pins was used as a single probe with sweeping frequency of 1 kHz, and the other four gave two floating potential measurements (V_f) and an ion saturation current (I_s) measurement, which were used to study the electrostatic fluctuation properties and the electrostatic radial particle flux. One of the two V_f measurements was obtained from two electrically connected pins located on either side of the pin measuring I_s , so that the V_f and I_s measurements can be considered to be taken at the same location. The two V_f measurements were 44 mm toroidally apart. The fluctuation data were sampled at 1 MHz. All the measurements were made keeping the probes on the head side protected with respect to the unidirectional superthermal electron flow which is found in the edge of RFP plasmas [9].

The plasma potential, from which the radial electric field was derived, is obtained as $V_p = V_f - \alpha T_e$ where T_e is the electron temperature. The factor α , calculated neglecting the secondary electron emission and taking into account the different collection surfaces for electrons and ions has been estimated to be $\alpha = -2.5$ [10]. Figure 1 shows the plasma potential and the corresponding $\mathbf{E} \times \mathbf{B}$ velocity as a function of the normalized radius r/a (the $r/a = 1$ surface is identified as that where the floating potential measured with respect to the first wall vanishes). As described elsewhere [3] two naturally occurring velocity shear layers can be identified. The first one is located across the plasma boundary, at $r/a > 0.97$. The shear is of the order of 10^6 s^{-1} , similar to that found in tokamaks and stellarators across the last closed flux surface [5]. The second velocity shear is more internal, at $r/a < 0.97$. This second shear has been already noticed to remind observations of tokamak plasmas in L or H mode [8], and to increase with plasma current, being typically 10^6 s^{-1} at a plasma current of 300 kA [3]. This Letter is focused on the role of this second velocity shear in the decorrelation of the electrostatic turbulence.

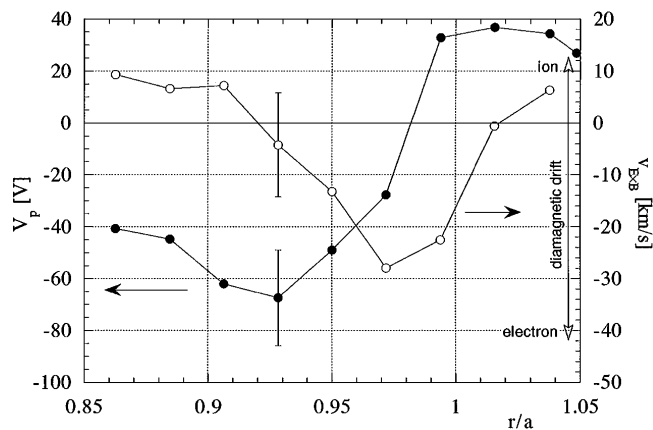


FIG. 1. Radial profiles of plasma potential and $\mathbf{E} \times \mathbf{B}$ drift velocity. Each point is an average over multiple shots. A typical error bar is plotted, which gives the standard deviation of the data.

The radial particle flux induced by the electrostatic turbulence Γ_{es} has been evaluated from two-point measurements according to the usual expression [11]

$$\Gamma_{es} = \frac{2}{B} \int_0^\infty k_\perp(\omega) \tilde{n}(\omega) \tilde{\phi}(\omega) \gamma_{n\phi}(\omega) \sin \alpha_{n\phi}(\omega) d\omega, \quad (1)$$

where B is the mean magnetic field, \tilde{n} and $\tilde{\phi}$ are the square root of the auto power spectra of density and plasma potential fluctuations, $\gamma_{n\phi}$ is the coherence between density and plasma potential, $\alpha_{n\phi}$ is their relative phase, and k_\perp is the transverse wave number of the plasma potential fluctuations. Fluctuations of ion saturation current and floating potential have been assumed to represent the fluctuations of density and plasma potential, thus neglecting temperature fluctuations. The coherence between V_f and I_s is high, with values ranging from 0.4 to 0.6 over the whole explored frequency range. The floating potential fluctuation amplitude is typically $e\delta V_f/T_e \sim 1.5$.

The dots in Fig. 2 show the measured Γ_{es} radial profile. The maximum, found around $r/a = 0.97$, is in agreement with the hydrogen influx measured on a chord viewing the edge plasma in the outer equatorial region, which, in turn, by averaging on the whole plasma surface, gives a particle confinement time of the order of 1 ms. Thus, like in most RFP devices, in RFX the particle flux at the edge is found to be driven by electrostatic fluctuations, at least at low plasma current. The consistency between the electrostatic particle flux obtained with the approximations reported above and the particle flux derived from H_α measurements confirms that the contribution of temperature fluctuations can be neglected. The flux measurements have been also compared with a model which simulates the ionization of hydrogen neutrals coming from the first wall [12]. The curves depicted in Fig. 2 show the computed source of hydrogen ions and the related particle flux. The code, which takes as inputs the experimental temperature and

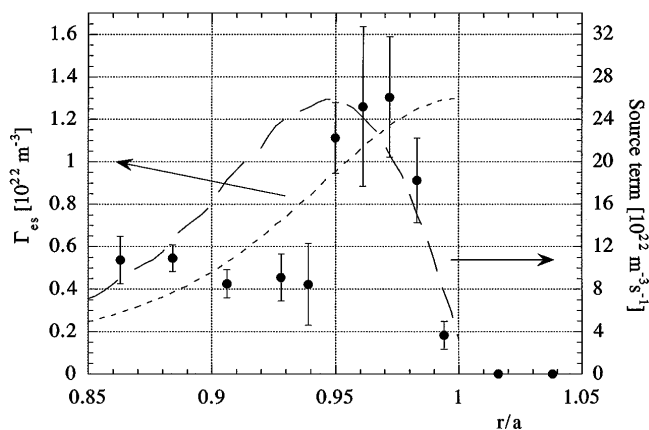


FIG. 2. Radial profile of the particle flux driven by electrostatic fluctuations (black dots). Each point is an average over multiple shots, with error bars showing the standard error. On the same graph two curves are shown which represent the particle flux and the related source term predicted by a numerical model.

density profiles, gives results in substantial agreement with the experimental data. The good agreement also in terms of particle flux radial profile offers further support to the approximations made in evaluating the particle flux.

For completeness, it must be noted that the particle flux decay in the region $r/a > 0.98$ is similar to that found in other experiments [2]. It can be attributed to relative position uncertainties between probe tips and last closed flux surface or to the wall proximity, which affects the particle balance by parallel losses to the wall due to plasma column shift, field errors or MHD instabilities.

The density profile, measured in the same discharges with a single Langmuir probe is shown in Fig. 3. From the density gradient $\nabla n = 6 \times 10^{20} \text{ m}^{-4}$, almost constant in the region $0.86 < r/a < 1$, it is straightforward to calculate the particle diffusion coefficient D assuming a Fick's diffusion law, i.e., $\Gamma_{es} = -D\nabla n$. It is found that $D \approx 20 \text{ m}^2/\text{s}$ in the region where the particle flux has a

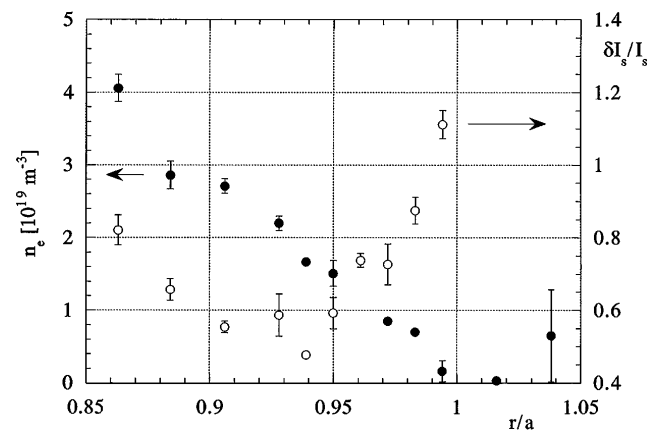


FIG. 3. Profiles of electron density n_e and ion saturation current fluctuation level $\delta I_s/I_s$. Each point is an average over multiple shots, with error bars showing the standard error.

peak, whereas it is between 5 and 10 m²/s for 0.86 < r/a < 0.94.

The results of the numerical simulation shown in Fig. 2 indicate that, due to the high density gradient in the outer plasma, the source term is concentrated in the outer 20% of the minor radius. Thus the decrease of the particle flux at $r/a \leq 0.94$ depends mainly on the source reduction. Nonetheless, the comparison of the diffusion coefficient profile with the $\mathbf{E} \times \mathbf{B}$ velocity shown in Fig. 1 leads to the observation that the particle diffusion is maximum where the velocity shear is small, and decreases going deeper into the plasma, in the region of the second velocity shear. The question arises whether the $\mathbf{E} \times \mathbf{B}$ velocity shear can actually play a role in the transport reduction for $r/a \leq 0.94$.

In order to investigate the influence of the velocity shear on the flux and diffusion coefficient profiles, other features of the electrostatic turbulence have been studied. The ion saturation current fluctuation level $\delta I_s/I_s$ is plotted in Fig. 3 as a function of the normalized radius r/a . A minimum is found at $r/a = 0.94$, in the middle of the second velocity shear region. Indeed, theory predicts that a velocity shear can decrease the fluctuation level if it is strong enough to decorrelate the turbulence [7]. In the same region the relative phase between V_f and I_s does not change significantly, whereas their squared coherence γ^2 (averaged over the particle flux power spectrum) is found to decrease as shown in Fig. 4. These observations suggest that the shear flow could be an important mechanism for edge turbulence [13]. It is worth noting that also the k_\perp spectrum seems to be affected. Indeed, the k_\perp averaged over the V_f power spectrum is minimum around the position $r/a = 0.94$, where it is equal to 12 m⁻¹. This estimate is reliable since the phase velocity is different from zero, even where the $\mathbf{E} \times \mathbf{B}$ velocity vanishes.

Since there are some elements suggesting a possible effect of the second velocity shear layer on the electrostatic turbulence, a quantitative test has been attempted in order

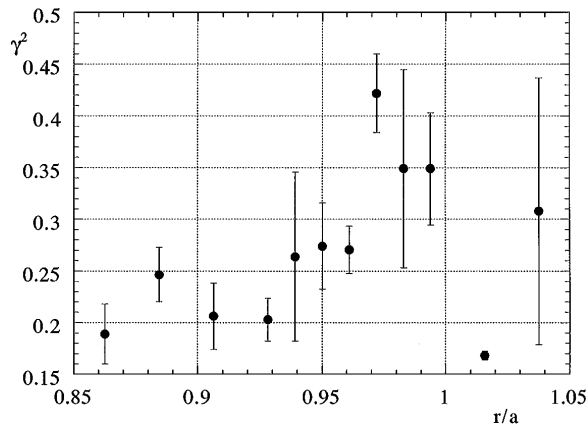


FIG. 4. Squared coherence between V_f and I_s averaged over the particle flux power spectrum. Each point is an average over multiple shots, with error bars showing the standard error.

to check if the velocity shear is strong enough to induce such an effect. According to the Biglari-Diamond-Terry (BDT) model [7], the turbulence can be radially decorrelated by the velocity shear if the shearing frequency ω_s ($\omega_s = k_\perp \Delta r_t dv_{\mathbf{E} \times \mathbf{B}}/dr$, where $dv_{\mathbf{E} \times \mathbf{B}}/dr$ is the radial derivative of the $\mathbf{E} \times \mathbf{B}$ velocity and Δr_t is the ambient turbulence radial correlation length) is larger than the ambient turbulence spectrum width $\Delta \omega_t$. Such decorrelation is expected to yield a reduced turbulence level and a decrease in the associated transport. The BDT model has been applied to the region of high velocity shear ($r/a = 0.94$). In this region $dv_{\mathbf{E} \times \mathbf{B}}/dr$ is equal to $(1.1 \pm 0.4) \times 10^6$ s⁻¹. The values of k_\perp and $\Delta \omega_t$, computed as averages over the floating potential power spectrum, are (12 ± 2) m⁻¹ and $(3.3 \pm 0.3) \times 10^5$ rad/s, respectively. These numbers imply that, for the velocity shear to be strong enough to decorrelate the turbulence, the ambient radial correlation length should be larger than (2.5 ± 1.0) cm. In making the comparison it is important to bear in mind that the measured radial correlation length Δr_m should be lower than the ambient value Δr_t , if the decorrelation process is indeed in action. The measurement of Δr_m has been made with the reflectometer, as described in the following.

The microwave reflectometer operating on RFX is an homodyne type with a single horn antenna [14] and has been recently upgraded to obtain an ultrafast sweep rate (up to 4 GHz/ μ s) in the Ka band. The reflectometer has been operated in O-mode, sweeping the range 34–38 GHz in 1 μ s (corresponding to densities between 1.4 and 1.8 $\times 10^{19}$ m⁻³), with a repetition rate of 1.25 μ s. To determine the radial correlation length, the reflected microwave power P_{ni} at different probing frequencies f_i is obtained from the intermediate frequency signal. Although the sweeping rate is very high, a correction is needed to account for the decorrelation introduced by the different times at which the measurements for different frequencies are made. The autocorrelation time τ for a given density has been measured using sequences of sweeps made at a reduced frequency span (35.5–36.5 GHz) with a repetition rate of 250 ns, alternated by the measurements at full range sweep. Typical values of τ have been found in the range 0.5–0.8 μ s.

The apparent radial correlation density N' , estimated directly from the decay of the correlation between couples of reflected power signals $P_{ni}P_{nj}$ for different density intervals $\Delta n = n_i - n_j$, can be approximated by an exponential:

$$C'(\Delta n) = \frac{\langle P_{ni}(t)P_{nj}(t) \rangle}{\sqrt{\langle P_{ni}^2(t) \rangle \langle P_{nj}^2(t) \rangle}} = \exp\left(-\frac{\Delta n}{N'}\right). \quad (2)$$

Upon assuming that the correlation function for both time and density intervals may be written as

$$C(\Delta n, \Delta t) = \exp\left(-\frac{\Delta n}{N} - \frac{\Delta t}{\tau}\right), \quad (3)$$

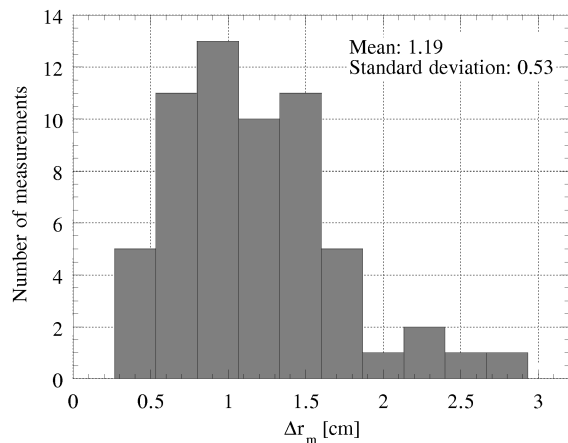


FIG. 5. Histogram showing the distribution of the measured values of the density fluctuation radial correlation length Δr_m .

the effective correlation density N can be found by means of the relationship

$$N = N' \left(1 - \frac{N'}{\tau dn/dt} \right)^{-1} \quad (4)$$

where the instrumental factor dn/dt ($0.4 \text{ m}^{-3}/\mu\text{s}$) is the reflectometer sweep rate in the given density range. Finally, the radial correlation length is calculated dividing the radial correlation density by the density gradient measured from Langmuir probes: $\Delta r_m = N/(dn/dr)$. It must be noted that, according to some authors [15], the correlation length determined in this way could be underestimated by a factor around 1.5.

The distribution of the radial correlation length measurements obtained with the technique described above in the region around $r/a = 0.94$ is shown in Fig. 5. The average value is 1.2 cm, with a standard deviation of 0.5 cm. The obtained value is, within the error bars, close to the condition required for the BDT decorrelation mechanism to apply. As pointed out above, the value in the absence of velocity shear could be greater than this. It can thus be concluded that in RFX at low plasma current the naturally occurring $\mathbf{E} \times \mathbf{B}$ velocity shear is close to that required for radial decorrelation of the electrostatic turbulence.

For completeness, it must be mentioned that the second derivative (curvature) of the $\mathbf{E} \times \mathbf{B}$ velocity can have a stabilizing effect [8]. In the present case, such an effect is negligible in the second velocity shear layer, around $r/a = 0.94$, where the BDT criterion has been applied. On the

other hand, curvature induced stabilization could be significant around the minimum of the $v_{\mathbf{E} \times \mathbf{B}}$ profile ($r/a = 0.97$), and will be the object of future investigation.

In conclusion, the work presented herein shows for the first time that the particle flux at the edge of RFX is mainly driven by electrostatic fluctuations, as found in tokamaks, stellarators and most of RFP experiments. Furthermore, a decorrelation process related to the naturally occurring $\mathbf{E} \times \mathbf{B}$ velocity shear has been inferred to be acting or close to apply to these fluctuations, since in the shear layer the I_s fluctuation level and the coherence are reduced and so is the related particle diffusivity. The analogy with the same mechanism acting in the tokamak H mode suggests the possibility for RFPs of achieving regimes of improved particle confinement by enhancing the plasma rotation through external means.

The authors wish to thank Dr. D. Gregoratto and Dr. L. Garzotti for the neutral influx simulations and Dr. M. E. Puiatti and Dr. L. Carraro for providing the H_α data.

-
- [1] V. Antoni, Plasma Phys. Controlled Fusion **39**, B223 (1997).
 - [2] A. J. Wootton *et al.*, Phys. Fluids B **2**, 2879 (1990).
 - [3] V. Antoni, D. Desideri, E. Martines, G. Serianni, and L. Tramontin, Phys. Rev. Lett. **79**, 4814 (1997).
 - [4] A. Möller, in *Proceedings of the 24th EPS Conference on Controlled Fusion and Plasma Physics, Berchtesgaden, 1997* (EPS, Geneva, 1997), Part III, p. 1273.
 - [5] H. Y. W. Tsui *et al.*, Phys. Fluids B **5**, 2491 (1993).
 - [6] B. E. Chapman *et al.*, Phys. Rev. Lett. **80**, 2137 (1998).
 - [7] H. Biglari, P. H. Diamond, and P. W. Terry, Phys. Fluids B **2**, 1 (1990).
 - [8] K. H. Burrell, Phys. Plasmas **4**, 1499 (1997).
 - [9] Y. Yagi, V. Antoni, M. Bagatin, D. Desideri, E. Martines, G. Serianni, and F. Vallone, Plasma Phys. Controlled Fusion **39**, 1915 (1997).
 - [10] V. Antoni, M. Bagatin, D. Desideri, E. Martines, and G. Serianni, Nucl. Fusion **36**, 435 (1996).
 - [11] S. J. Levinson, J. M. Beall, E. J. Powers, and R. D. Bengston, Nucl. Fusion **24**, 527 (1984).
 - [12] D. F. Duchs, D. E. Post, and P. H. Rutherford, Nucl. Fusion **17**, 565 (1977).
 - [13] C. Hidalgo *et al.*, Nucl. Fusion **31**, 1471 (1991).
 - [14] M. Moresco, O. Dubhghaill, and E. Spada, Int. J. Infrared Millim. Waves **12**, 609 (1992).
 - [15] G. D. Conway, Plasma Phys. Controlled Fusion **39**, 407 (1997).